RESEARCH PAPER

A novel fabrication of PVA/Alginate-Bioglass electrospun for biomedical engineering application

Aliasghar Saberi [1], Mohammad Rafienia [2], Elahe Poorazizi [3]*

[1]Department of Tissue Engineering, Najafabad Branch, Islamic Azad University, Najafabad, Iran

[2]Biosensor Research Center, Isfahan University of Medical Sciences, Isfahan, Iran

[3]Department of Biochemistry, Najafabad Branch, Islamic Azad University, Najafabad, Iran

ABSTRACT

Objecttive (s): Polyvinylalcohol (PVA) is among the most natural polymers which have interesting properties such as nontoxic nature, biodegradability and high resistance to bacterial attacks making it applicable for tissue scaffolds, protective clothing, and wound healing.

Materials and Methods: In the current work, PVA and Na-Alginate nanocomposite scaffolds were prepared using the electrospinning (ELS) technique in an aqueous solution. Also, (5% and 10%) addition of bioglass (BG) ceramic to the nanocomposite scaffold were investigated. The blended nanofibres are characterized by scanning electron microscopy (SEM), Fourier-transform infrared (FTIR), also the bioactivity evaluation of nanocomposite scaffold performed in simulated body fluid (SBF) solutions.

Results: The FTIR analysis indicated that PVA and Alginate may have H+ bonding interactions. The results revealed that with a higher amount of BG, a superior degradation as well as a higher chemical and biological stability could be obtained in the nanobiocomposite blend fibres. Furthermore, the blend nanofibre samples of 10% BG powders exhibit a significant improvement during bioactivity and mechanical testing.

Conclusion: The increasing water-contact angle on the polymer surface with decreasing PVA and Alginate content indicated that the scaffold were more hydrophobic than were PVA molecules. Also, In addition, the average diameter of fibers in the sample with 10% BG have the highest porosity compared to the other scaffold samples.

Keywords; *Alginate, Bioglass, Electrospinning, Polymer, Tissue Engineering*

INTRODUCTION

There has been an interesting attention in biodegradable and nonbiodegradable polymers materials proposed for nanomedicine applications [1-2]. To produce excellent soft/hard scaffolds, the important properties are proper biological, mechanical, chemical stability, great porosity, and a condition that allow the cells organisms to grow and proliferate on the surface of the tissue [3]. It is well recognized that micropores fibers have suitable interconnectivity and can play significant rule in the growth cellular on the bone and help the regeneration of tissues [4]; however, improving the fibers porosity is occurring with decreasing

* Corresponding Author Email: m_rafienia@med.mui.ac.ir,

the mechanical properties. Therefore, various types of polymers like poly vinylalcohol (PVA) [5, 23], poly acrylamide (PAC) [6], and poly acrylicacid (PAA)[7]have been evaluated for soft/hard artificial tissue application by several researchers. Among the investigated polymers, PVA has been implemented for nanomedicine applications better than other polymers [8-12]. The PVA has interesting properties like suitable nontoxicity, hydrophilicity, food safe degradation, mechanical properties, biocompatibility, high degradation in water, and bioadhesive characteristic. The PVA can applied for regenerative medicine especially wound skin healing, optical, chemical destruction and degradation products which are excreted without any harm to the body [13-15]. Another

known polymer, alginate is used to mix with nanomaterials to enhance the behaviour of based polymers. In addition, the alginate has been used as an emulsifier, pharmaceutical products and wound healing applications [15]. The alginate and PVA represent renewable sources and do not have adverse impact on skin and eye irritation. It is known that alginate have proper ductility, commercial availability and high efficiency that will facilitate manufacturing capabilities [16-17]. In this study, the nanocomposite PVA/alginate/bioaglass (PVA/Alg/BG) is reconstructed. Notwithstanding the weak mechanical properties of polymer materials, the excellent biology behavior of BG and alginate attracts our attention to focus on enhancing the properties of the PVA polymer for biomedical application. The BG bioceramics has recently been taken into consideration due to its good chemical and mechanical stability. Adding BG to biopolymer-based nanocomposites improves their mechanical, biological, chemical, thermal properties of polymers [18-21]. The electrospinning (ELS) technique common used method of making polymer scaffolds for tissue engineering approaches. ELS technique is simple, economic and commercializes method in biomaterials field for preparation of soft tissues [22-24]. The polymer fibers prepared by ELS technique have excellent mechanical properties, flexibility and biocompatibility inside the human's body. Therefore, we have prepared a novel PVA/Alg/BG nanocomposite for the first time as a bioactive material for wound healing applications.

MATERIALS AND METHODS

Starting materials poly vinylalcohol (PVA) (M_w=145,000) (Merck Co, Germany), Alginate (Aldrich Co., USA) and bioglass (BG) (Nikceram, Iran Co.) were purchase. The chemistry analysis of bioglass were assessed with X-ray fluorescence (XRF) test and represented in Table 1.

Table 1. XRF quantitative analysis of the composition (wt%) of BG nanoparticles ceramics

Component	(wt%)
SiO_2	55
CaO	35
P_2O_5	6.5
Ag_2O	3.5
Impurity	0.05

Composite Preparation

Four polymer scaffold nanocomposite solution were prepared with different ratios 100, 90:10, 85:10, and 80:10 of PVA/Alginate in 100 ml of deionized water. The BG particles with 5% and 10% (w/w) were added to the nanocomposite solutions. The influence of BG on the biopolymers was investigated by FTIR and SEM analysis that equipped by EDX software. The BG powder was then slowly added to the PVA/Alginate solution on stirrer at room temperature (T=37°C). The solution was allowed to mix for 1 h in a sealed container and then obtained mixture was further sonicated for 20 min.

Electrospinning Technique

The prepared scaffold nanocomposite solution were separately added by dispersion of PVA and Alginate in distilled water and then stirred. Then, ELS technique as one of the most important approaches for developing continuous nanoscale fibres with diameters ranging from 10-50 nm were used to the sample. Each sample solutions were mixed with PVA solution at constant volume ratio. The prepared solutions were applied into a 5 mL syringe of ELS tools as represented in schematic Fig 1. The condition for ELS were selected at room temperature (T=37°C) according to the procedure described by Heydari et al. [1, 8]. The feed rate setting for ELS adjusted at 0.25 mL/h. Then the nanofiber nanocomposite scaffolds produced on aluminum foil rotated drum. The collector distance from tip of needle set at 15-20 cm. The adequate high voltage was choosing at 15 with step of 5 kV. The optimum voltage observed to select was 25 kV. Also, the dimension of frame was 10×50 mm² which was positioned at a constant distance of 10 cm from the needle. Finally, the prepared scaffolds dried at 50-60°C in the vacuum condition for removing the moisture and the residual solvent of scaffolds. The ELS procedure (compositing (PVA, Alginate, and BG), syringe pump, and electrospun on aluminum foil) is shown in Fig. 1.

Biological Testing
Bioactivity Test

To recognize the biological response of scaffold nanocomposite the specimen are soaked in the simulated body fluids (SBF). According to the Kokubo's test, the important requirement for any materials to mimic and bond with the host tissue can be recognized by the formation of

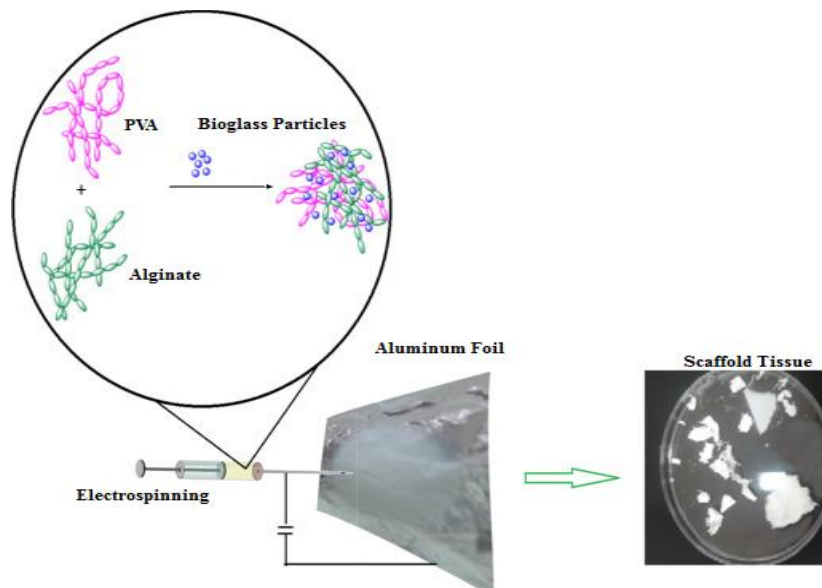*Nanomed. J. 4(3): 152-163, Summer 2017*

153

Fig. 1. Schematic of electrospinning of PVA/Alg-BG scaffold for tissue engineering
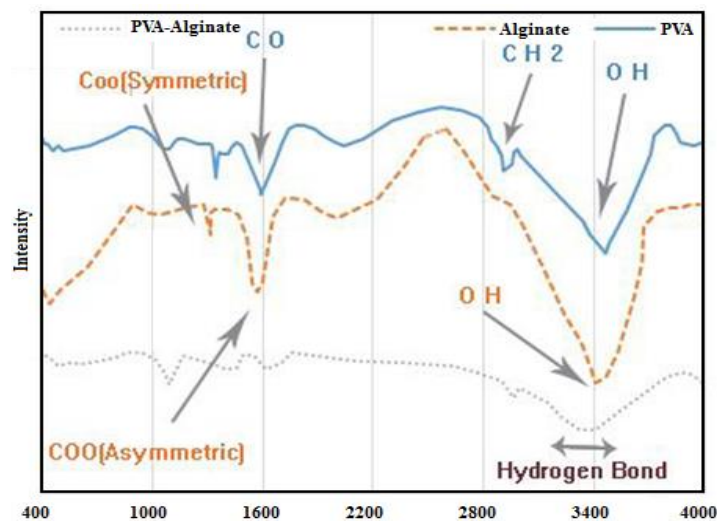

Fig. 2. FTIR spectra for PVA, Alginate, and PVA/Alginate scaffolds nanofibre

apatite (bone-like/cauliflower) on its surface after the implantation to the live part [25-28]. The formation of apatite on the surface of scaffold nanocomposite of polymer/bioglass show proper ability to precipitate apatite (cauliflower) on the surface of samples [28-30]. Table 2 shows the SBF ion concentration solution according to the Kokubo's test and the comparison of SBF with human blood plasma. The SBF were fabricated according to the procedure described by Kokubo et al. [31]. In this study, the nanocomposite scaffold samples were immersed in the SBF solution for the certain period times of 1, 2, and 3 weeks at 37°C with pH = 7.4 to investigate bioactivity and biodegradation of samples. The samples were dried for 45 min at 50°C after the soaking in the SBF and weighted to record the weight changes (weight loss).

Weight loss test

The degree of the weight loss of the nanofibre samples was calculated by the use of Eq. (1). The test is carried out in the phosphate buffered saline, PBS (pH=7.4) at 37°C for 1, 2, and 3 weeks. The PBS

154

Nanomed. J. 4(3): 152-163, Summer 2017

solution was prepared by dissolving the NaCl (8 g), KCl (0.2 g), Na_2HPO_4 (1.44 g), and KH_2PO_4 (0.24 g) in 800 ml deionized water according to the Table 2. The pH of PBS prepared at room temperature has to be adjusted at 7.4. The nanocomposite scaffolds were inserted in a 20 ml falcon tube with 15 ml PBS solution. The produced samples were then placed in sonicate water bath at 37 ±1 °C for 3 weeks. Each week, the solution pH was measured by pH metre. Weight change was calculated by this formula

$$\text{Swelling ratio(\%)} = \frac{w - w0}{w0} \times 100 \qquad (1)$$

W_0 = initial dry weight sample and W_t = dry weight sample after specific time.

Mechanical properties

The PVA/Alginate nanocomposite scaffold with 5% and 10% BG nanoparticles were tested for mechanical testing. The mechanical properties of fibres including tensile strength and elongation at fracture point are measured by tensile machine.

Characterization of materials
Fourier Transform Infrared Spectroscopy (FTIR) Analysis

The nanocomposite scaffolds were investigated with FTIR spectra. All spectrums were taken at room temperature on a spectrometer with spectral range of 4000–400 cm^{-1} and 4.0 cm^{-1} resolution. Spectra were performed for PVA, Alginate, and PVA/Alginate scaffolds nanofibre containing 10% wt. BG. To evaluate the chemical composition changes of nanofibres the FTIR (Perkin-Elmer, UK) was used.
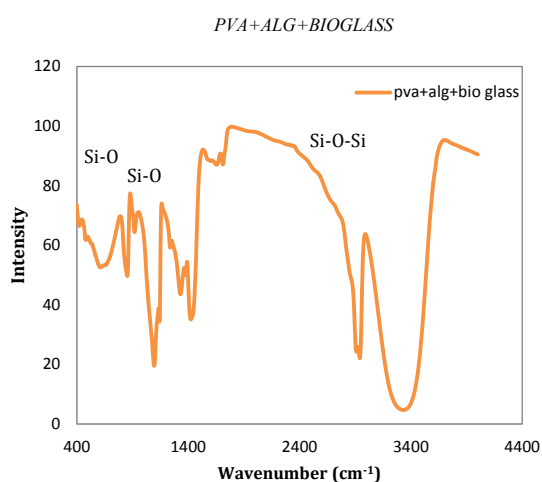
PVA+ALG+BIOGLASS

Fig. 3. FTIR spectra of the PVA/Alginate- with 10% amount of BG powder in nanocomposite scaffold

Morphology of electrospun nanofibers analysis

The surface morphology and diameter of the electrospun nanofibers were investigated with a scanning electron microscope (SEM; Philips XL30, Netherlands). Small sections of Al foil which coated with electrospun nanofibers was cut and sputter coated with gold to prevent electron charging. All of the samples were coated with gold (Au) using spraying, high vacuum and 40 kV accelerating voltage.

Inductive coupled plasma atomic emission Spectroscopy (ICP-OES) Analysis

The concentrations of Ca, Si, and P ions in SBF after soaking were determined using inductive coupled plasma atomic emission spectroscopy (ICP-AES) with Zaies (110394c).

RESULTS AND DISCUSSION
FTIR Analysis

FTIR spectra were also recorded for PVA and Alginate and PVA/Alginate nanocomposite (see Fig. 2). The characteristic band at 3442 cm^{-1} was detected for the stretching frequency of --OH groups as shown in Fig. 2. Asymmetric and symmetric stretching vibrations for methylene groups appeared at around 2940 cm^{-1}. A significant band at 1500-1600 cm^{-1} is attributed to –C=O group stretching vibrations. The strong peak at 1243 cm^{-1} is attributed to stretching vibrations of C-O groups (Fig. 2). The bands around 2925 and 2854 cm^{-1} 1 are assigned to asymmetric and the symmetric stretching to -CH$_2$ group, respectively. Two peaks at 1737 and 1434 cm^{-1} can be observed for to -CO stretching vibrations: -OH and -CH bending respectively. Heydari et al. [1] investigate a novel type of Gum and nanoclay bioceramic mixed (with PVA solutions. In their work the spectra of PVA/Gum/Nanoclay blend nanofibre, the absorption peak at 1617 cm^{-1} was assigned to asymmetrical stretch of —COO$^-$ group which appeared at 1594 cm^{-1} for Gum and shifted to 1618 cm^{-1} for Gum/PVA nanofibre, suggesting that most of the carboxylic acid groups were associated with intramolecular hydrogen bonding.

PVA contains only single bonds therefore would be expected to absorb radiation only in the far UV (120–200 nm). The two absorption bands at 250-350 nm are probably due to carbonyl functionalities. Also, the FTIR spectra of scaffold nanocomposite PVA/Alginate containing 10%wt. BG represented in Fig. 3.

Nanomed. J. 4(3): 152-163, Summer 2017

155

Table 2. Comparison of nominal ion concentrations of SBF, physiological saline, and human blood plasma

composition (g l^{-1})	Artificial blood	PBS	SBF
KH$_2$PO$_4$	--	0.2	--
NaCl	6.8	8.0	8.035
KCl	0.4	0.2	0.225
CaCl$_2$.H$_2$O	0.2	--	--
NaH$_2$PO$_4$.H$_2$O	0.026	--	--
Na$_2$HPO$_4$.H$_2$O	0.126	--	--
MgSO$_4$	0.1	--	--
NaHCO$_3$	2.2	--	0.355
Na$_2$HPO$_4$	--	1.15	--
MgCl$_2$.6H$_2$O	--	--	0.311
K$_2$HPO$_4$.3H$_2$O	--	--	0.231
Na$_2$SO$_4$	--	--	0.072
CaCl$_2$	--	--	0.292
HCl (1.0 mol l^{-1})	--	--	39 ml
Tris-hydroxymethylamino	--	--	
Methane	--	--	6.118
pH	7.4	7.4	7.2-7.4

SEM analysis

SEM photomicrographs of the PVA/Algnano-composite powders (100, 90.10 samples) at different percentages (%5 and In the sample fibre of 80/10 with 10% BG, the uniform, randomly oriented nanofibres were obtained. Such fibrous structure would result in high mechanical and biological properties. A comparison between the SEM images of the sample in the presence and without BG is shown in Fig 4. It is seen that irregular surface morphologies were obtained by adding the BG powders (see Fig. 4-d). Investigation of sample containing PVA/Alg-10% BG shows randomly oriented nanofibres in the matrix compared to the sample without BG nanoparticles (see Fig. 4 (a-b) and 4 (c-d)). Such fibrous structure would result in a high amount of the surface area to volume ratio and interconnected porosity.

Bioactivity evaluation

The SEM and EDX micrograph of nanocomposite scaffolds in Fig 5 (a-d) shown that the density of fibers increased after 28 days of soaking in the SBF solution. Also, the nanocomposite scaffold containing 10% of BG had the cauliflower and bone-formation in the maximum of possible amount. The maximum amount of bone-like apatite formation is due to stable state of the BG nanoparticles powder in the SBF solution.

As it is seen in Fig 5, there are heavy and mass agglomerates particles that created in the nanocomposite scaffold with higher percentage of BG (see Fig. 5-d). The chemical stability of nanofiber increased with adding BG nanoparticles into the nanocomposite scaffold. It seem that that the agglomeration decreased by adding the BG nanoparticles. The result arises from the accumulation of brittle ceramic phases as a consequence of increasing BG amount.

Adding more than 5% BG leads to more pile of nanoparticles in polymer structure resulting in the reduction of mechanical features. SEM micrographs explain that the blend fibres have a shorter diameter pattern in the presence of more amount of BG. All the scaffold nanocomposite soaked in SBF solution were characterized by EDX analysis to recognize the presence of the elements on their surface (Fig. 5). EDX results on the large white tiny particle indicate that it include mainly oxygen, sodium, magnesium, phosphorus, chlorine, calcium, carbon and silicon. The carbon peak on the EDX analysis comes from the PVA as well as the Alginate. White tiny spots on the EDX maps represent the cite with maximum concentrations of the studied elements, and also proved the occupancy of apatite formation. Dissolution curves can be very helpful in this area that indicates the changes in weight of nanocomposite scaffold values versus immersion time in SBF (see Fig. 6). Also, the EDX analysis show there is amount of Na, P, Ca, and K in the tiny agglomerate scaffold sample. As the samples soaked in the SBF for long period of time, the rate of bioactivity decreased. The alteration in BG nanoparticles amount leads to higher AAS in the scaffold samples. The scaffold absorbs the calcium ions from the first week up to the last week. The highest rate of bioactivity dedicate to the

156

Nanomed. J. 4(3): 152-163, Summer 2017

Table 3. Samples mechanical (Avg. Porosity, tensile strength, elastic module, length) and biological properties (water absorption, bioactivity rate)

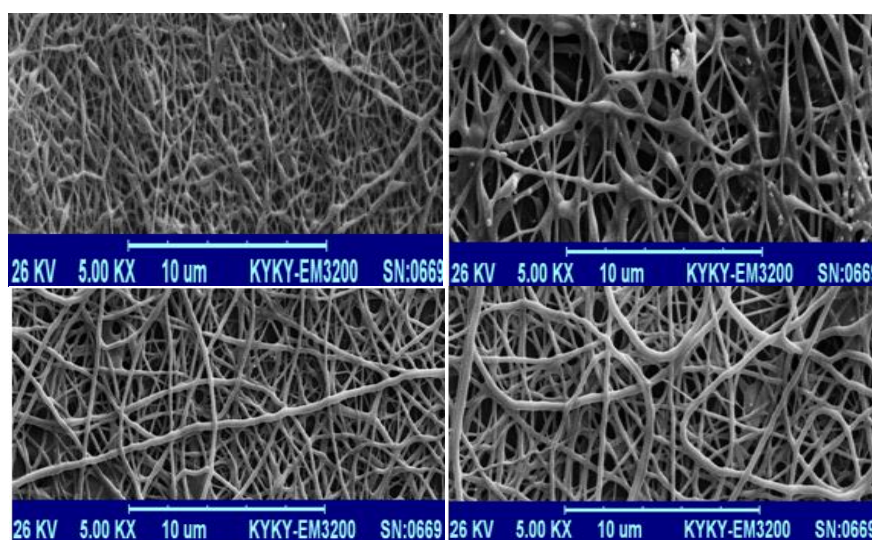| Polymer Composition	Ratio	Water absorption	Avg. porosity (µm)	Fiber diameter (nm)	Tensile strength (Mpa)	Elastic module (MPa)	Length change (mm)
PVA	100	0.13	63	81.63	8.1	15	1.6
PVA-Alg	90-10	0.15	72.1	162.4	20.5	17.2	1.2
PVA-Alg-BG	90-10-0.05	--	89.3	182.66	12.5	18	1.05
PVA-Alg-BG	80-10-10	0.17	105.9	233.1	--	--	0.8

Fig. 4. SEM Images of electrospun (a) PVA, (b) PVA/Alginate, (c) PVA/Alginate-5% BG, and (d) PVA/Alginate-10% BG

sample with higher amount of BG nanoparticles. The research studies show that four scaffold nanocomposite PVA/Alginate/BG prepared by ELS technique. The surface characterization of the mineral phase of bone HA showed high ability to produce cauliflower and tiny agglomerate particles. It can be concluded, the formation of apatite on scaffolds surface must be considered [25-27].Here we try to calculate the amount of atomic absorption using calcium ions content examination. In the present case, the density of the pellet material is much higher as compared to that of the trabecular bone and upon foaming they may well match to further confirms this, the density of the foam materials was calculated and the average density of the foam scaffolds was found to be 0.92 g/cm³. Once present in the body, the material is expected to start degrading and will lead to further decrease in the density of the material due to the increase in the size and number of pores. Therefore, the density is low enough to mimic the trabecular bone whose density lies in the range of 0.09–0.75 g/cm³.

Rate of degradation and time of degradation is important in design of soft and hard tissue materials [3-10]. Because the degradation rate of scaffold is plan, then the host tissue faced with high stress and tension around the area. Also, in the high degradation rate the cells are not able to recover and growth adequately. Another important is that when the degradation is occurred, the additional and waste materials should be removed easily. Fig 6 show the degradation rate of scaffolds prepared in this work. Due to the regeneration of bone is 0.02 a year and the required generation time 45 days, the prepared scaffold should have proper surface degradation rate. According what is described in this section scaffold should degrade bone up to 5-10% in the first month. The investigation of scaffold showed that the pure PVA has lower degradation rate. The lower degradation rate of PVA is because of hydrophobicity (see Fig. 7) and lower porosity of these scaffolds [1, 5, and 32]. The sample with higher amount of BG have

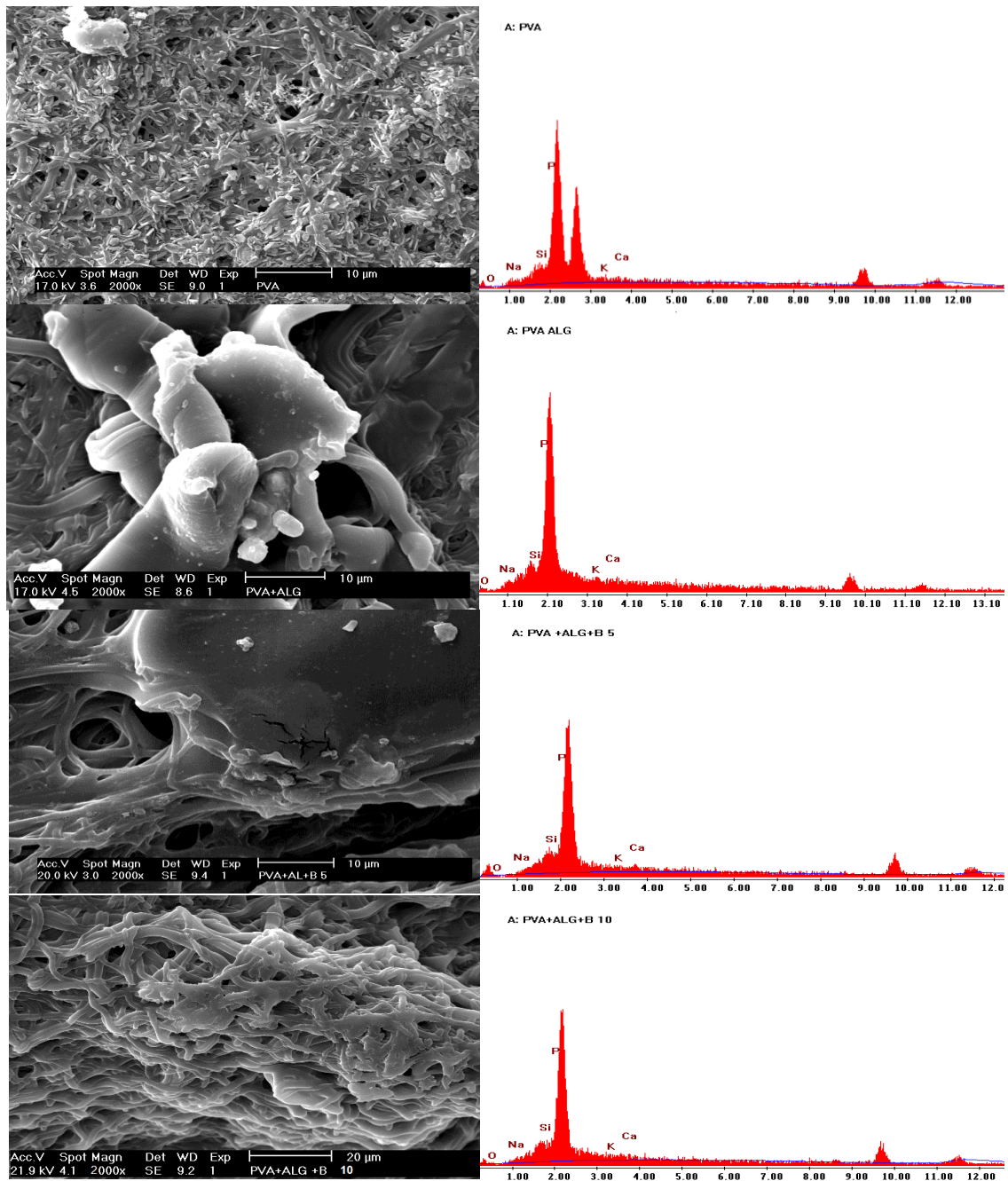*Nanomed. J. 4(3): 152-163, Summer 2017*

157

Fig. 5. SEM and EDX images of (a) PVA, (b) PVA/Alginate, (c) PVA/Alginate-5% BG, and (d) PVA/Alginate-10% BG nanocomposite scaffold

better hydrophobicity compared to the sample without BG nanoparticles as shown in Fig 7 (a) and 7(c). The degradation rate of sample containing 10% BG have slower slope compare to the sample without BG particles. Also, the AAS results are measured using water absorption by formula (3-1). In the case of adding alginate to PVA the water absorption amount increased from 13% to 15% which leads to higher porosity of the scaffolds. On the other hand, adding 10% BG particles the porosity increased to 17%. Researchers investigated the PVA/Alginate/Hydroxyapatite (PVA/Alg/HA) with various content of alginate [33-34]. It is possible to use other CaPs and silicate
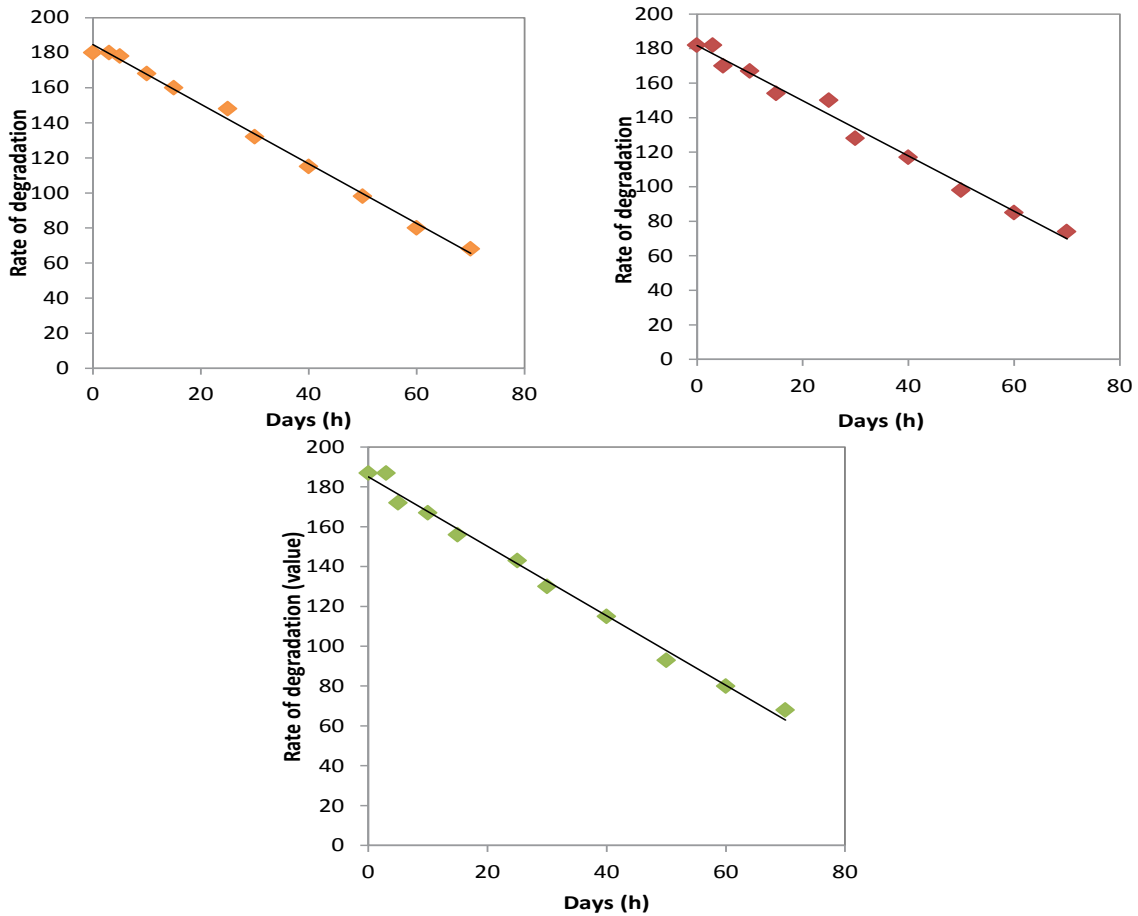
Fig. 6. Degradation rate of PVA, PVA/Alginate, and PVA/Alginate-Bioglass nanocomposite scaffold

bioceramics to PVA/Alg like baghdadite [35], akermanite [36-37], diopside [26], TCP [32], and Flurohydroxyapatite (FHA) [27]. They showed that after 3days the scaffold sample without alginate and sample with the highest amount of alginate have the maximum degradation rate. In our study, the SEM images showed that addition of alginate increase the fiber diameter.

ICP-AES analysis
The ICP results indicate that as a number of BG increases, the weight loss starts to decline. Generally, bioceramics improve the chemical stability and mechanical properties of the polymers. Fig. 6 shows the curve of PVA/Alg-BG nanofibres containing different amount of BG after degradation for a period of 28 days. The increase of degradation rate in the nanocomposite samples is due to this fact that the BG acts as filler between the polymer bonding and so it improves the capability of microorganism growth, and subsequently easier and faster destruction of polymer structure.

Mechanical properties
Mechanical properties of biopolymers typically investigated by adding some ceramic or metallic particles to enhance the strength and hardness. Recently, polymers are produced in the nano and macro-scale. In this study, the BG and Alginate added to PVA polymer matrix. The proposed of adding bioglass ceramic is the high elastic modulus of ceramic compared to the elastic modulus of polymer materials. Adding alginate to the PVA leads to a higher elastic modulus of PVA. The increase in elastic modulus is related to hydrogen bonding among the PVA and alginate materials. The hydrogen bonding leads to the massive
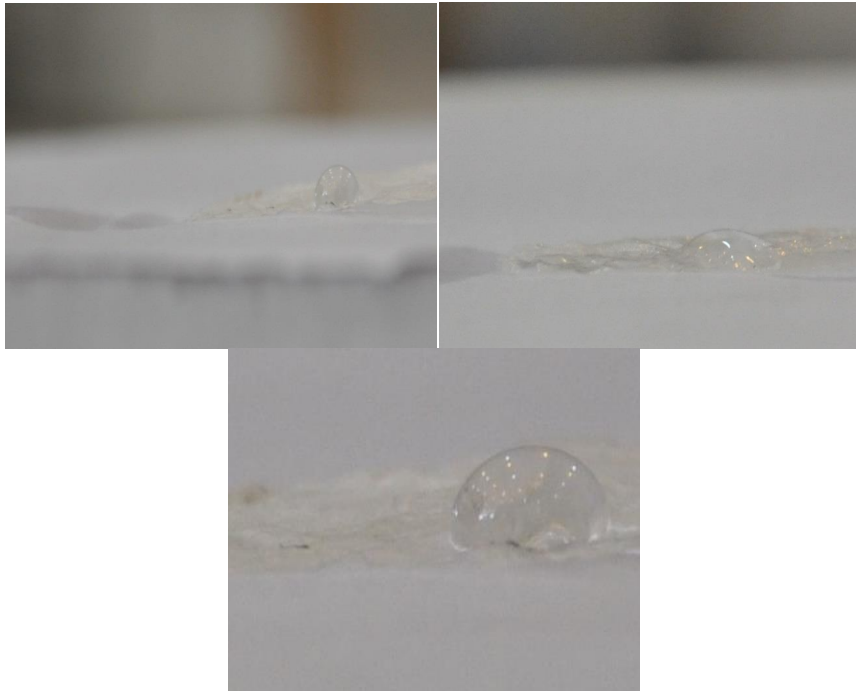
Nanomed. J. 4(3): 152-163, Summer 2017

159

Fig. 7. Images of PVA (a) electrospun, (b) PVA/Alginate (c) PVA/Alginate-10%BG

reduction in the compressive strength of PVA/Alginate nanocomposite scaffold compared to pure PVA scaffold sample. Although the BG particles do not produce active chemical bonding and added for increasing the physical performance, the BG nanoparticles lead to higher elastic modulus and decrease in compressive strength in PVA/Alg-BG compared to the sample without BG content. As the young modulus of spongy bone is 15-100 MPa it seems that PVA/Alg-BG is likely to spongy bone and can be suitably addressed to apply for bone tissue engineering applications. Scaffolds composed of Alginate, chitosan, and collagen show potential applicability to use for general bulking agents [14, 37-38]. The mechanical property results of PVA, PVA/Alg, and PVA/Alg-BG blend nanofibres are compared in Fig. 8. As can be seen, the tensile strength and elongation at fracture have increased with increasing BG amount compared to the pure PVA sample. This approach indicates that there are specific intermolecular interactions between BG and PVA/Alg. However, the tensile strength and elongation in the sample PVA/Alginate are about 20-25 MPa. Heydari et al. [1 ,32], indicate that adding nanoclay to the PVA/Gum can enhance the mechanical properties of PVA/Gum-NC blends, they have found that their nanocomposite

samples shape clear homogeneous blends in comparison with those in PVA/Gum [1, 8]. This is probably because of the more Young's modulus as well as tensile stress in the later samples. Silicate additive like akermanite, baghdadite, diopside, and bredigite can enhanced the mechanical and chemical properties of polymer materials [39]. In recent years, chitosan, cellulose, gums and their applications in the field of tissue engineering
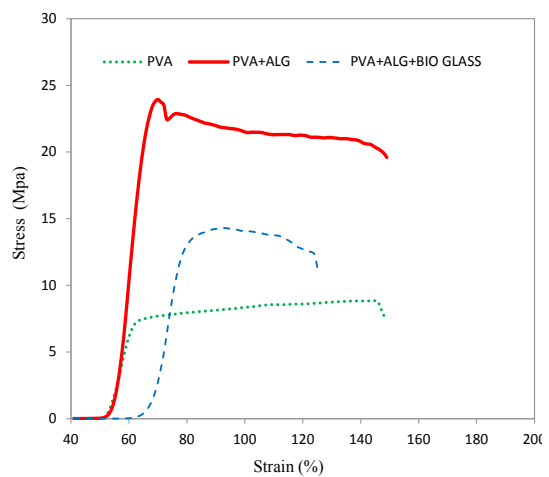

Fig. 8. Stress–strain diagram of PVA, PVA/Alg nanofibres, and PVA/Alg-10% BG nanocomposite scaffold

160

Nanomed. J. 4(3): 152-163, Summer 2017

have attracted considerable attention. It has been studied as a useful biomaterial in diverse tissue engineering applications because of its hydrophilic surface that promotes cell adhesion, proliferation and differentiation, good biocompatibility and host response, biodegradability by lysozyme and other enzymes, bactericidal/bacteriostatic activity, and the capacity to maintain a predefined shape after cross-linking [40-43].

CONCLUSION

In the current study the novel PVA/Alginate-BG nanocomposite prepared by electrospun with proper biological and mechanical properties for soft/hard tissue applications. The results indicated that a PVA/Alginate added with 10% BG could electrospun homogenises nanofibres. The mixed nanofibres present better mechanical properties compared to the pure electrospun PVA. The FTIR and SEM results showed that there were strong interactions between BG ceramic and PVA/Alginate. All biological properties of PVA/Alginate-10% BG scaffolds were suitably addressed. Alginate components were found to be concentrated on the surface of the air-surface side of the PVA/Alginate blends as the alginate is more hydrophobic than PVA. The SEM images showed that scaffold with 10% BG have regular and proper flexibility rather than other samples without BG ceramic powder. Also, by adding the BG ceramic powder the fibers diameter increased more than three times (from 81.6 to 233.1 nm) in the sample containing 10% BG bioceramic powder. In addition, the average diameter of fibers in the sample with 10% BG has the highest porosity compared to the other scaffold samples.

ACKNOWLEDGEMENTS

CONFLICT OF INTEREST

The authors confirm that this article content has not any conflicts of interest.

REFERENCES

1. Heydary HA, Karamian E, Poorazizi E, Heydaripour J, Khandan A. Electrospun of polymer/bioceramic nanocomposite as a new soft tissue for biomedical applications. J As Cer S. 2015; 3(4): 417-425.

2. Nasri-Nasrabadi B, Mehrasa M, Rafienia M, Bonakdar S, Behzad T, Gavanji S. Porous starch/cellulose nanofibers composite prepared by salt leaching technique for tissue engineering. Carbohyd polym. 2014; 108: 232-238.

3. Webster TJ. Nanotechnology for the regeneration of hard and soft tissues. World Scientific; 2007.

4. Guarino V, Causa F, Taddei P, di Foggia M, Ciapetti G, Martini D, Fagnano C, Baldini N, Ambrosio L. Polylactic acid fibre-reinforced polycaprolactone scaffolds for bone tissue engineering. Biomaterials. 2008; 29(27): 3662-3670.

5. Peppas NA, Mongia NK. Ultrapure poly (vinyl alcohol) hydrogels with mucoadhesive drug delivery characteristics. Eur J pharm biopharm. 1997; 43(1): 51-58.

6. Varaprasad K, Vimala K, Ravindra S, Reddy NN, Raju KM. Development of sodium carboxymethyl cellulose-based poly(acrylamide-co-2acrylamido-2-methyl-1-propane sulfonic acid) hydrogels for in vitro drug release studies of ranitidine hydrochloride an anti-ulcer drug. Polym-Plast Techno. 2011; 50(12): 1199-1207.

7. Steiner G, Zimmerer C. Poly (acrylic acid)(PAA). Polymer Solids and Polymer Melts–Definitions and Physical Properties I. 2013; 527-533.

8. Heydary HA, Karamian E, Poorazizi E, Khandan A, Heydaripour J. A Novel Nano-Fiber of Iranian Gum Tragacanth-Polyvinyl alcohol/Nanoclay Composite for Wound Healing Applications. Procedia Materials Science. 2015; 11: 176-182.

9. Malarvizhi GL, Retnakumari AP, Nair S, Koyakutty M. Transferrin targeted core-shell nanomedicine for combinatorial delivery of doxorubicin and sorafenib against hepatocellular carcinoma. Nanomedicine: (N B M). 2014; 10(8): 1649-1659.

10. Boyer C, Whittaker MR, Bulmus V, Liu J, Davis TP. The design and utility of polymer-stabilized iron-oxide nanoparticles for nanomedicine applications. NPG Asia Materials. 2010; 2(1): 23-30.

11. Morton SW, Herlihy KP, Shopsowitz KE, Deng ZJ, Chu KS, Bowerman CJ, DeSimone JM, Hammond PT. Scalable Manufacture of Built-to-Order Nanomedicine: Spray-Assisted Layer-by-Layer Functionalization of PRINT Nanoparticles. Adv Mater. 2013 ; 25(34): 4707-4713.

12. Makhluf SB, Abu-Mukh R, Rubinstein S, Breitbart H, Gedanken A. Modified PVA–Fe3O4 nanoparticles as protein carriers into sperm cells. Small. 2008; 4(9): 1453-1458.

13. Hariharan R, Senthilkumar S, Suganthi A, Rajarajan M. Photodynamic action of curcumin derived polymer modified ZnO nanocomposites. Mater Res Bull. 2012; 47(11): 3090-3099.

14. Jayakumar R, Menon D, Manzoor K, Nair SV, Tamura H. Biomedical applications of chitin and chitosan based nanomaterials—A short review. Carbohyd Polym. 2010;

Nanomed. J. 4(3): 152-163, Summer 2017

161

82(2): 227-232.

15. George J, Sajeevkumar VA, Ramana KV, Sabapathy SN. Augmented properties of PVA hybrid nanocomposites containing cellulose nanocrystals and silver nanoparticles. J Mater Chem. 2012; 22(42): 22433-22439.

16. Gaur N, Flora G, Yadav M, Tiwari A. A review with recent advancements on bioremediation-based abolition of heavy metals. Environ. Sci.: Processes Impacts. 2014; 16(2): 180-193.

17. Skardal A, Atala A. Biomaterials for integration with 3-D bioprinting. Ann biomed eng. 2015; 43(3): 730-746.

18. Nazemi Z, Mehdikhani-Nahrkhalaji M, Nazarpak MH, Staji H. Antibacterial effect of bioactive glass nanoparticles prepared via sol gel method. J Kermanshah Univ Med Sci. 2014; 18(7): 381-387.

19. Mehdikhani-Nahrkhalaji M, Fathi MH, Mortazavi V, Mousavi SB, Hashemi-Beni B, Razavi SM, Akhavan A, Haghighat A. In Vivo and In Vitro Evaluation of Poly (lactide-co-glycolide)/Bioactive Glass Nanocomposite Coating. Adv Mat Res. 2014; 829: 309-313.

20. Day RM. Bioactive glass stimulates the secretion of angiogenic growth factors and angiogenesis in vitro. Tissue Eng. 2005; 11(5): 768-777.

21. Nazemi Z, Mehdikhani-Nahrkhalaji M, Haghbin-Nazarpak M, Staji H, Kalani MM. Antibacterial activity evaluation of bioactive glass and biphasic calcium phosphate nanopowders mixtures. Appl. Phys. A. 2016 ;122(12): 1063.

22. Koski A, Yim K, Shivkumar S. Effect of molecular weight on fibrous PVA produced by electrospinning. Materials Letters. 2004 Jan 31; 58(3): 493-497.

23. Doustgani A, Pedram MS. Preparation and investigation of polylactic acid, calcium carbonate and polyvinylalcohol nanofibrous scaffolds for osteogenic differentiation of mesenchymal stem cells. Nanomed j. 2016 ;3(2): 109-114.

24. Doustgani A. The effect of electrospun poly (lactic acid) and nanohydroxyapatite nanofibers' diameter on proliferation and differentiation of mesenchymal stem cells. Nanomed j. 2016; 3(4): 217-222.

25. Karamian E, Motamedi MR, Khandan A, Soltani P, Maghsoudi S. An in vitro evaluation of novel NHA/zircon plasma coating on 316L stainless steel dental implant. PNS: M I. 2014; 24(2): 150-156.

26. Khandan A, Abdellahi M, Ozada N, Ghayour H. Study of the bioactivity, wettability and hardness behaviour of the bovine hydroxyapatite-diopside bio-nanocomposite coating. J Taiwan Ins Chem Eng. 2016; 60: 538-546.

27. Karamian E, Abdellahi M, Khandan A, Abdellah S. Introducing the fluorine doped natural hydroxyapatite-titania nanobiocomposite ceramic. J Alloy Compd. 2016; 679: 375-383.

28. Kazemi A, Abdellahi M, Khajeh-Sharafabadi A, Khandan A, Ozada N. Study of in vitro bioactivity and mechanical

properties of diopside nano-bioceramic synthesized by a facile method using eggshell as raw material. Mater Sci and Eng: C. 2017; 71: 604-610.

29. Stamboulis AG, Boccaccini AR, Hench LL. Novel biodegradable polymer/bioactive glass composites for tissue engineering applications. Adv Eng Mater. 2002; 4(3): 105-109.

30. Xu H, Lv F, Zhang Y, Yi Z, Ke Q, Wu C, Liu M, Chang J. Hierarchically micro-patterned nanofibrous scaffolds with a nanosized bio-glass surface for accelerating wound healing. Nanoscale. 2015; 7(44): 18446-18452.

31. Kokubo T, Takadama H. How useful is SBF in predicting in vivo bone bioactivity. Biomaterials. 2006; 27(15): 2907-2915.

32. Khandan A, Ozada N, Karamian E. Novel Microstructure Mechanical Activated Nano Composites for Tissue Engineering Applications. J Bioeng Biomed Sci. 2015; 5(1): 1.

33. Tolba E, Abd-Elhady BM, Elkholy B, Elkady H, Eltonsi M. Biomimetic synthesis of guided-tissue regeneration hydroxyapatite/polyvinyl alcohol nanocomposite scaffolds: influence of alginate on mechanical and biological properties. J Am Sci. 2010; 6: 239-249.

34. Karamian E, Khandan A, Eslami M, Gheisari H, Rafiaei N. Investigation of HA nanocrystallite size crystallographic characterizations in NHA, BHA and HA pure powders and their influence on biodegradation of HA. Adv Mat Res. 2014; 829: 314-318

35. Najafinezhad A, Abdellahi M, Ghayour H, Soheily A, Chami A, Khandan A. A comparative study on the synthesis mechanism, bioactivity and mechanical properties of three silicate bioceramics. Mater Sci Eng: C. 2017; 72: 259-267.

36. Sharafabadi AK, Abdellahi M, Kazemi A, Khandan A, Ozada N. A novel and economical route for synthesizing akermanite (Ca 2 MgSi 2 O 7) nano-bioceramic. Mater Sci Eng: C. 2017; 71: 1072-1078.

37. Khandan A, Abdellahi M, Barenji RV, Ozada N, Karamian E. Introducing natural hydroxyapatite-diopside (NHA-Di) nano-bioceramic coating. Ceram Int. 2015; 41(9): 12355-12363.

38. Taranejoo S, Janmaleki M, Rafienia M, Kamali M, Mansouri M. Chitosan microparticles loaded with exotoxin A subunit antigen for intranasal vaccination against Pseudomonas aeruginosa: an in vitro study. Carbohyd polym. 2011; 83(4): 1854-1861.

39. Khandan A, Karamian E, Mehdikhani-Nahrkhalaji M, Mirmohammadi H, Farzadi A, Ozada N, Heidarshenas B, Zamani K. Influence of spark plasma sintering and baghdadite powder on mechanical properties of hydroxyapatite. Proc Mat Sci. 2015; 11: 183-189.

40. Beladi F, Saber-Samandari S, Saber-Samandari S. Cellular compatibility of nanocomposite scaffolds based on hydroxyapatite entrapped in cellulose network for bone

162

Nanomed. J. 4(3): 152-163, Summer 2017

repair. Mat Sci Eng C. 2017; 75: 385-392.

41. Saber-Samandari S, Saber-Samandari S. Biocompatible nanocomposite scaffolds based on copolymer-grafted chitosan for bone tissue engineering with drug delivery capability. Mat Sci Eng C. 2017; 75: 721-732.

42. Abd-Khorsand S, Saber-Samandari S, Saber-Samandari S. Development of nanocomposite scaffolds based on TiO 2 doped in grafted chitosan/hydroxyapatite by freeze drying method and evaluation of biocompatibility. Int J Biol Macromol. 2017; 101: 51-58.

43. Zare-Harofteh A, Saber-Samandari S, Saber-Samandari S. The effective role of akermanite on the apatite-forming ability of gelatin scaffold as a bone graft substitute. Ceram Int. 2016; 42(15): 17781-1791.

Nanomed. J. 4(3): 152-163, Summer 2017

163